

# Electron and hole polarons at the BiVO<sub>4</sub>-water interface

Julia Wiktor\* and Alfredo Pasquarello

*Chaire de Simulation à l'Echelle Atomique (CSEA), Ecole Polytechnique Fédérale de  
Lausanne (EPFL), CH-1015 Lausanne, Switzerland*

E-mail: [julia.wiktor@epfl.ch](mailto:julia.wiktor@epfl.ch)

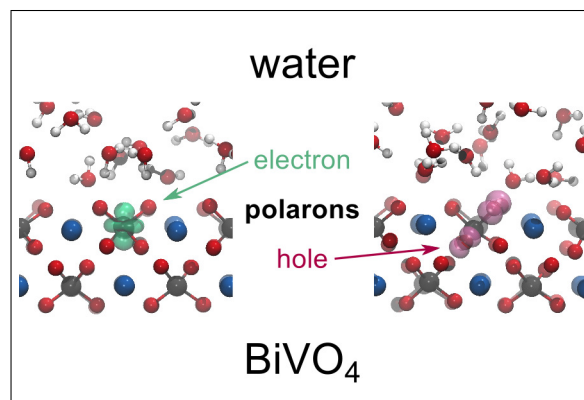
---

\*To whom correspondence should be addressed

## Abstract

We determine the energy levels of hole and electron polarons at the  $\text{BiVO}_4$ -water interface through hybrid functional molecular dynamics and thermodynamic integration, thereby accounting for the liquid nature of the water component. The electron polaron is found to be less stable at the interface than in the bulk by 0.18 eV, while for the hole polaron the binding energy increases by 0.20 eV when the charge localizes in the surface layer of  $\text{BiVO}_4$ . These results indicate that interfacial effects on the polaron binding energy and charge distribution are sizeable and cannot trivially be inferred from bulk calculations.

## Graphical TOC Entry



Photocatalytic water splitting is a promising technique to transform solar energy into fuel in the form of hydrogen. In a water-splitting cell, photogenerated electrons and holes originating from a photoabsorber drive  $\text{H}^+$  reduction and  $\text{H}_2\text{O}$  oxidation. These reactions occur at the semiconductor-water interface, therefore their efficiency is affected by the processes occurring at the interface.

Bismuth vanadate has emerged as a promising photoanode for water-splitting photoelectrochemical cells,<sup>1-4</sup> due to its band gap allowing for the absorption of a substantial portion of the visible light, and the favorable position of the band edges with respect to the water redox potentials. The bulk properties of  $\text{BiVO}_4$  have been the subject of numerous computational studies.<sup>5-8</sup> However, since the water-splitting reaction occurs at the interface with water, the material surface and the presence of the solvent strongly impact the relevant phenomena. It has previously been shown that the electron and hole in bulk  $\text{BiVO}_4$  localize forming polarons.<sup>9</sup> These states introduce transition levels within the band gap and thus affect the band alignment with the water redox levels. However, it can be expected that the polaronic levels in the bulk and at the interface differ, e.g., due to the occurrence of broken bonds in the latter case.

In this Letter, we study electron and hole polarons at the  $\text{BiVO}_4$ -water interface through the use of an atomistic interface model that accounts for the thermal motion of the water molecules. The molecular dynamics (MD) simulations are carried out at the hybrid functional level to properly describe the localization of excess holes and electrons at the interface. The polaron binding energies are then consistently determined through the thermodynamic integration method within the same theoretical scheme. Our work reveals the energy levels and the charge localization of interfacial electron and hole polarons in comparison with their bulk counterparts.

To study polarons at the  $\text{BiVO}_4$ -water interface, we perform molecular dynamics simulations using the hybrid functional PBE0,<sup>10</sup> which allows one to treat the self-interaction error<sup>11-13</sup> and to describe localized electronic states.<sup>14</sup> In the PBE0 functional, we set the

mixing parameter  $\alpha$  to 0.22. Such functional, after taking into account various corrections affecting the electronic structure of  $\text{BiVO}_4$ , such as spin-orbit coupling, thermal, and quantum effects, reproduces well the experimental band gap of about 2.6 eV.<sup>8</sup> This choice is based on the fact that a hybrid functional reproducing the correct band gap of a semiconductor is also capable of describing polaronic distortions, as shown by Miceli *et al.*<sup>14</sup> We describe van der Waals (vdW) interactions through the non-local rVV10 functional.<sup>15</sup> The empirical parameter  $b$  of the rVV10 functional is set to 7.7 to reproduce the experimental density of water for the employed hybrid functional. This value is based on the interpolation of results from Refs. 16 and 17, where the optimal  $b$  parameter was determined for  $\alpha = 0$  and  $\alpha = 0.40$ . The MD simulations are performed with the CP2K code<sup>18</sup> in the canonical  $NVT$  ensemble at a temperature of 350 K. This temperature is chosen to achieve frank diffusive motion of water. We note that this temperature differs from the one used in our previous study on bulk polarons in  $\text{BiVO}_4$  (300 K).<sup>9</sup> However, by extrapolating the temperature effect on the bulk polarons found in the previous study from 300 K to 350 K linearly we find that the results at these two temperatures should differ by about 35 meV. Therefore, the results on the interface polarons presented in this work can be compared with the levels calculated in the bulk. The orbitals are described with atom-centered Gaussian-type basis functions and the electron density is re-expanded with an auxiliary plane-wave basis set. We use double- $\zeta$  MOLOPT basis sets<sup>19</sup> for Bi, O, and V. For H, a triple- $\zeta$  basis set is employed. The cut-off energy is set to 600 Ha for the plane waves. Core-valence interactions are described by Goedecker-Teter-Hutter pseudopotentials.<sup>20</sup>

We model the  $\text{BiVO}_4(010)$ -water interface with an orthorhombic supercell ( $a = 10.39$ ,  $b = 10.18$ , and  $c = 36.17$  Å) containing a six-layer semiconductor slab and 56 water molecules. We approximate the  $\beta$  angle of the  $C2/c$  monoclinic structure to  $90^\circ$ . The employed slab is symmetric, therefore the two interfaces are equivalent. A representative configuration of the studied system is given in the Supporting Information (Fig. S1). The MD are initiated with equilibrated configurations taken from previous simulations of the considered system.<sup>21,22</sup> We

sample the Brillouin zone at the  $\Gamma$  point. The time step is set to 0.5 fs and the simulations are evolved for about 5 ps. We study hole and electron polarons by removing or adding one electron to the supercell. In these cases, we perform spin-polarized calculations. We introduce initial distortions in the first layer of the  $\text{BiVO}_4$  slab, to avoid polaron formation in the bulk region. Since the CP2K code does not include spin-orbit effects and only allows for  $\Gamma$ -point sampling of the Brillouin zone, we correct the positions of the band edges of  $\text{BiVO}_4$  using the results of Ref. 8. We neglect finite-size corrections in the calculations,<sup>23-25</sup> due to the high dielectric constants of  $\text{BiVO}_4$  ( $\epsilon_0=68$ )<sup>26</sup> and water ( $\epsilon_0=78.3$ ).<sup>27</sup> We calculate the transition levels corresponding to the localized charges at the  $\text{BiVO}_4$ -water interface through the thermodynamic integration (TI)<sup>28</sup> method. Further details on the TI calculations of the transition levels can be found in the Supporting Information (SI). We note that in the case of hole and electron polarons, the binding energies  $E_b$  (energies of localized charges relative to those of free states) can be directly related to the transition levels  $\mu$ . For the electron this relationship reads  $E_b^{\text{el}} = \epsilon_c - \mu_{\text{el}}$  and for the hole  $E_b^{\text{h}} = \mu_{\text{h}} - \epsilon_v$ , where  $\epsilon_c$  and  $\epsilon_v$  are the positions of the conduction and valence band edges, respectively.

We first analyze the results for the electron polaron. The representative instantaneous isodensity of the electron polaron at the interface is shown in the Fig. 1. We compare the interface polaron with its bulk counterpart.<sup>9</sup> The same distribution of localized charge can be noticed in the two cases. The electron localizes at a single V atom, changing its ionization state from +5 to +4 through the occupation of an empty  $3d$  orbital. The  $d$ -orbital shape can be clearly recognized in Fig. 1. Through thermodynamic integration, we find the transition level associated with the electron polaron to lie 0.70 eV below the conduction band minimum of  $\text{BiVO}_4$ . In Fig. 2, we align the transition level of the electron polaron at the interface with respect to its bulk level, the band edges of  $\text{BiVO}_4$ , and the  $\text{H}^+/\text{H}_2$  and  $\text{H}_2\text{O}/\text{O}_2$  redox levels. The alignment of these levels relies on data from Ref. 9 and is illustrated for  $\text{pH} = 7$ . In Ref. 9, a binding energy of 0.88 eV was found for the bulk polaron. This means that the binding energy of the electron polaron at the interface is by 0.18 eV lower than in the bulk.

To understand the lower binding energy of the electron polaron at the interface, we analyze the geometry of the  $\text{VO}_4$  unit in which the charge is localized. We show in Fig. 3 the vanadium-oxygen radial distribution function  $g_{\text{V-O}}(r)$  for the cases of charged and neutral  $\text{VO}_4$  units, in the bulk and at the interface. First, one notices that the trapping of an electron leads to the expansion of the V-O bonds both in the bulk and at the interface. Second, we observe a distribution with a single peak in the bulk and one with a double peak at the interface, both in presence and absence of polaron trapping. This means that the  $\text{VO}_4$  unit is asymmetrically distorted at the interface with the V-O bonds oriented towards the surface being shorter than those oriented towards bulk. The larger delocalization of the polaron associated with this symmetry breaking provides an explanation for the lower stability of the polaron at the interface. We also investigate the effect of the water molecules on the electron polaron at the interface, by examining a randomly chosen configuration. The calculation is described in the Supporting Information. We find that in the absence of water, the electron polaron is even less stable at the surface (binding energy by about 0.4 eV lower as compared with the bulk energy) and that water molecules stabilize the localized charge by about 0.2 eV. We note that the lower stability of the electron polaron at the surface was also noticed in a recent study of Mo and W doped  $\text{BiVO}_4$ .<sup>29</sup>

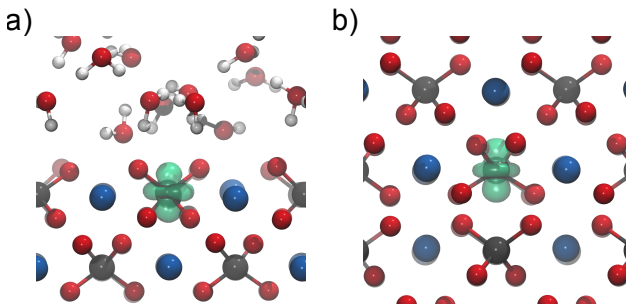


Figure 1: Isodensities of the electron polaron (a) at the  $\text{BiVO}_4$ -water interface and (b) in bulk  $\text{BiVO}_4$ .

Next, we focus on the hole polaron at the interface. In Fig. 4, the isodensity of an instantaneous configuration of the hole polaron at the  $\text{BiVO}_4$  surface is shown and compared

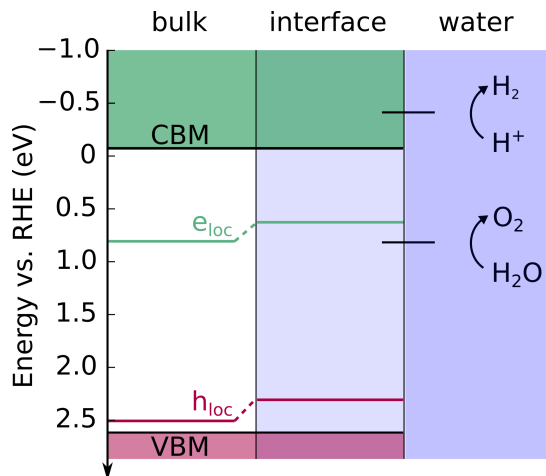


Figure 2: Alignment of the polaron transition levels in bulk  $\text{BiVO}_4$  and at the interface with the  $\text{H}^+/\text{H}_2$  and  $\text{O}_2/\text{H}_2\text{O}$  redox levels at  $\text{pH} = 7$ .

with the typical one of the bulk.<sup>9</sup> Unlike for the electron polaron, the distribution of localized charge of the hole strongly differs between the bulk and the interface. In the bulk, the charge is distributed over one bismuth and eight oxygen atoms. At the surface, the hole is mostly shared among two oxygen atoms neighboring an interfacial vanadium atom. Due to the charge localization, the distance between the two O atoms reduces to 2.29 Å on average, compared to the value of 2.78 Å observed between oxygen pairs in units of  $\text{VO}_4$  at the interface. We attribute the different localization of the hole at the interface and in the bulk to the fact that formation of a bond between two oxygen atoms is energetically more favorable than partial localization on eight atoms. In the bulk, however, interactions with other atoms keep two oxygen atoms apart and prevent the formation of such a bond, while at the interface one of the oxygen atoms can move more freely. We note that while the present study focuses on single charges, the localization of two holes and formation of a double bond between two oxygen atoms ( $\text{O}_2^{2-}$  anion) could lead to further charge stabilization. From the radial distribution function in Fig. 5, one notices no significant change in the V-O bond lengths within the  $\text{VO}_4$  unit. However, a second feature around 2.3 Å is observed in the  $g_{\text{V-O}}(r)$ . This peak corresponds to a displacement of one oxygen atom belonging to a  $\text{VO}_4$  unit in the second layer towards the localized charge.

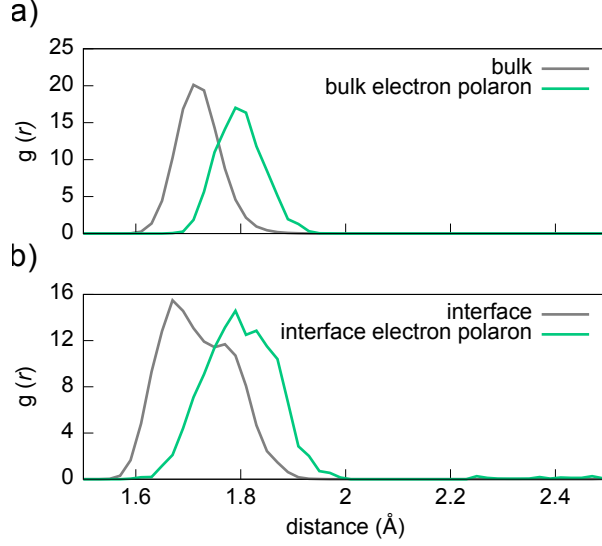


Figure 3: V-O radial distribution functions in a) bulk  $\text{BiVO}_4$  and b) at the  $\text{BiVO}_4$ -water interface with and without the electron polaron.

The stronger polaron localization of the hole polaron at the interface leads to a higher binding energy compared to the bulk case. Through thermodynamic integration, we find that the transition level associated with the localized hole at the interface lies at 0.31 eV from the valence band maximum, to be compared with the binding energy of 0.11 eV found in the bulk.<sup>9</sup> The energy levels of the hole polaron have been included in Fig. 2.

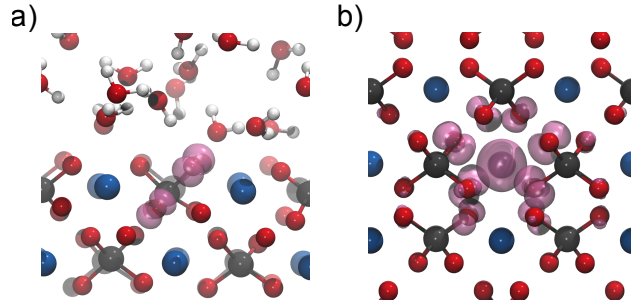


Figure 4: Isodensities of the hole polaron (a) at the  $\text{BiVO}_4$ -water interface and (b) in bulk  $\text{BiVO}_4$ .

Our results have implications for the modelling of materials in water-splitting devices, as well as for on-going materials searches. First, we have shown that the energetics of the polaronic states at the interface and in the bulk differ significantly. This means that



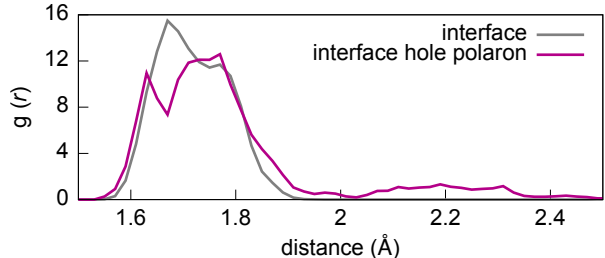


Figure 5: V-O radial distribution functions at the  $\text{BiVO}_4$ -water interface with and without the hole polaron.

the alignment of the energy levels at the  $\text{BiVO}_4$ -water interface cannot trivially be inferred from bulk calculations. Second, in the case of the hole polaron, we observe that its charge distribution undergoes significant change at the surface of the semiconductor. Therefore, bulk models of polarons in complex oxides might not even give qualitative insight into the charge localization occurring at the interface. This highlights the importance of modeling the interface explicitly for understanding the redox processes in water splitting cells, which is a fundamental aspect in the searches for new photoanode materials. Finally, our results show that the hole is most stable at the surface of  $\text{BiVO}_4$ , while the electron preferentially localizes deeper in the bulk. This spatial separation between electron and holes is expected to reduce the recombination rate between photogenerated charges and could lie at the origin of the high photocatalytic performance of bismuth vanadate.<sup>30</sup>

In conclusion, we analyze the role of the  $\text{BiVO}_4$ -water interface in the localization of excess charges. We combine thermodynamic integration and hybrid functional molecular dynamics to calculate the transition levels related to the hole and electron polarons at the interface. We find that the binding energy of the interfacial electron polaron amounts to 0.70 eV, lower than the bulk value of 0.88 eV. We attribute the electron polaron destabilisation to the lower localization induced by the distorted  $\text{VO}_4$  units at the interface. For the hole polaron, we show that the charge distribution undergoes significant change at the interface. While the hole localizes within a  $\text{BiO}_8$  unit in the bulk, the charge density is mostly shared among only two oxygen atoms at the interface. The stronger localization at the interface

leads to a deeper transition level at 0.31 eV above the valence band maximum. Our results highlight the importance of accounting for interfacial effects when addressing the localization and the energetics of excess charges in complex oxides.

## Acknowledgement

We thank Francesco Ambrosio for the models of the BiVO<sub>4</sub>-water interface. The authors acknowledge financial support from the Swiss National Science Foundation (SNSF) (Grant No. 200020-172524). This work has been realized in relation to the National Center of Competence in Research (NCCR) “Materials’ Revolution: Computational Design and Discovery of Novel Materials (MARVEL)” of the SNSF. We used computational resources of CSCS and SCITAS-EPFL.

## References

- (1) Kudo, A.; Omori, K.; Kato, H. A Novel Aqueous Process for Preparation of Crystal Form-Controlled and Highly Crystalline BiVO<sub>4</sub> Powder from Layered Vanadates at Room Temperature and Its Photocatalytic and Photophysical Properties. *J. Am. Chem. Soc.* **1999**, *121*, 11459–11467.
- (2) Yu, J.; Kudo, A. Effects of Structural Variation on the Photocatalytic Performance of Hydrothermally Synthesized BiVO<sub>4</sub>. *Advanced Functional Materials* **2006**, *16*, 2163–2169.
- (3) Luo, H.; Mueller, A. H.; McCleskey, T. M.; Burrell, A. K.; Bauer, E.; Jia, Q. Structural and Photoelectrochemical Properties of BiVO<sub>4</sub> Thin Films. *J. Phys. Chem. C* **2008**, *112*, 6099–6102.
- (4) Park, Y.; McDonald, K. J.; Choi, K.-S. Progress in bismuth vanadate photoanodes for use in solar water oxidation. *Chem. Soc. Rev.* **2013**, *42*, 2321–2337.

- (5) Walsh, A.; Yan, Y.; Huda, M. N.; Al-Jassim, M. M.; Wei, S.-H. Band Edge Electronic Structure of BiVO<sub>4</sub>: Elucidating the Role of the Bi *s* and V *d* Orbitals. *Chem. Mater.* **2009**, *21*, 547–551.
- (6) Zhao, Z.; Li, Z.; Zou, Z. Electronic Structure and Optical Properties of Monoclinic Clinobisvanite BiVO<sub>4</sub>. *Phys. Chem. Chem. Phys.* **2011**, *13*, 4746–4753.
- (7) Wadnerkar, N.; English, N. J. Density Functional Theory Investigations of Bismuth Vanadate: Effect of Hybrid Functionals. *Comput. Mater. Sci.* **2013**, *74*, 33–39.
- (8) Wiktor, J.; Reshetnyak, I.; Ambrosio, F.; Pasquarello, A. Comprehensive Modeling of the Band Gap and Absorption Spectrum of BiVO<sub>4</sub>. *Phys. Rev. Mater.* **2017**, *1*, 022401.
- (9) Wiktor, J.; Ambrosio, F.; Pasquarello, A. Role of Polarons in Water Splitting: The Case of BiVO<sub>4</sub>. *ACS Energy Letters* **2018**, *3*, 1693–1697.
- (10) Perdew, J. P.; Ernzerhof, M.; Burke, K. Rationale for Mixing Exact Exchange with Density Functional Approximations. *J. Chem. Phys.* **1996**, *105*, 9982–9985.
- (11) Zhang, Y.; Yang, W. A Challenge for Density Functionals: Self-Interaction Error Increases for Systems with a Noninteger Number of Electrons. *J. Chem. Phys.* **1998**, *109*, 2604–2608.
- (12) Pacchioni, G.; Frigoli, F.; Ricci, D.; Weil, J. A. Theoretical Description of Hole Localization in a Quartz Al Center: The Importance of Exact Electron Exchange. *Phys. Rev. B* **2000**, *63*, 054102.
- (13) Lægsgaard, J.; Stokbro, K. Hole Trapping at Al Impurities in Silica: A Challenge for Density Functional Theories. *Phys. Rev. Lett.* **2001**, *86*, 2834.
- (14) Miceli, G.; Chen, W.; Reshetnyak, I.; Pasquarello, A. Nonempirical hybrid functionals for band gaps and polaronic distortions in solids. *Phys. Rev. B* **2018**, *97*, 121112(R).

- (15) Sabatini, R.; Gorni, T.; de Gironcoli, S. Nonlocal Van Der Waals Density Functional Made Simple and Efficient. *Phys. Rev. B* **2013**, *87*, 041108.
- (16) Miceli, G.; de Gironcoli, S.; Pasquarello, A. Isobaric first-principles molecular dynamics of liquid water with nonlocal van der Waals interactions. *J. Chem. Phys.* **2015**, *142*, 034501.
- (17) Ambrosio, F.; Miceli, G.; Pasquarello, A. Structural, dynamical, and electronic properties of liquid water: A hybrid functional study. *J. Phys. Chem. B* **2016**, *120*, 7456–7470.
- (18) VandeVondele, J.; Krack, M.; Mohamed, F.; Parrinello, M.; Chassaing, T.; Hutter, J. Quickstep: Fast and Accurate Density Functional Calculations Using a Mixed Gaussian and Plane Waves Approach. *Comput. Phys. Commun.* **2005**, *167*, 103 – 128.
- (19) VandeVondele, J.; Hutter, J. Gaussian Basis Sets for Accurate Calculations on Molecular Systems in Gas and Condensed Phases. *J. Chem. Phys.* **2007**, *127*, 114105.
- (20) Goedecker, S.; Teter, M.; Hutter, J. Separable Dual-Space Gaussian Pseudopotentials. *Phys. Rev. B* **1996**, *54*, 1703–1710.
- (21) Ambrosio, F.; Wiktor, J.; Pasquarello, A. pH-dependent Catalytic Reaction Pathway for Water Splitting at the BiVO<sub>4</sub>-water Interface From the Band Alignment. *ACS Energy Lett.* **2018**, *3*, 829–834.
- (22) Ambrosio, F.; Wiktor, J.; Pasquarello, A. pH-dependent Surface Chemistry from First-Principles: Application to the BiVO<sub>4</sub>(010)-Water Interface. *ACS Appl. Mater. Interfaces* **2018**, *10*, 10011–10021.
- (23) Komsa, H.-P.; Rantala, T. T.; Pasquarello, A. Finite-Size Supercell Correction Schemes for Charged Defect Calculations. *Phys. Rev. B* **2012**, *86*, 045112.
- (24) Freysoldt, C.; Grabowski, B.; Hickel, T.; Neugebauer, J.; Kresse, G.; Janotti, A.; Van de

- Walle, C. G. First-Principles Calculations for Point Defects in Solids. *Rev. Mod. Phys.* **2014**, *86*, 253.
- (25) Komsa, H.-P.; Pasquarello, A. Finite-size supercell correction for charged defects at surfaces and interfaces. *Phys. Rev. Lett.* **2013**, *110*, 095505.
- (26) Wee, S.-H.; Kim, D.-W.; Yoo, S.-I. Microwave Dielectric Properties of Low-Fired ZnNb<sub>2</sub>O<sub>6</sub> Ceramics with BiVO<sub>4</sub> Addition. *J. Am. Ceram. Soc.* **2004**, *87*, 871–874.
- (27) Aki, S. N.; Brennecke, J. F.; Samanta, A. How polar are room-temperature ionic liquids? *Chem. Commun.* **2001**, 413–414.
- (28) Frenkel, D.; Smit, B. *Understanding Molecular Simulation: From Algorithms to Applications*; Academic Press, 2001; Vol. 1.
- (29) Cen, J.; Li, S.; Zheng, J.; Pan, F. Electron polarons in the subsurface layer of Mo/W-doped BiVO<sub>4</sub> surfaces. *RSC Advances* **2019**, *9*, 819–823.
- (30) Tokunaga, S.; Kato, H.; Kudo, A. Selective preparation of monoclinic and tetragonal BiVO<sub>4</sub> with scheelite structure and their photocatalytic properties. *Chem. Mater.* **2001**, *13*, 4624–4628.